



Cite this: *RSC Adv.*, 2020, **10**, 30186

Received 30th June 2020  
 Accepted 11th August 2020

DOI: 10.1039/d0ra05720g  
[rsc.li/rsc-advances](http://rsc.li/rsc-advances)

## A review on biological activities of Schiff base, hydrazone, and oxime derivatives of curcumin

Sakineh Omidi \* and Ali Kakanejadifard

Curcumin (1,7-bis[4-hydroxy-3-methoxyphenyl]-1,6-heptadiene-3,5-dione) is the main pigment present in the turmeric rhizome and shows various biological properties. The synthesis of different derivatives is an effective way to improve the medicinal and biological properties of curcumin. Many researchers have chosen the carbonyl group of curcumin for modification and preparation of new analogues. This review critically surveys a general overview of the literature and summarizes the synthesis and biological activities of Schiff base, hydrazone and oxime derivatives of curcumin over the last decade. These compounds and also their metal complexes possess higher potency in biological activity.

### 1. Introduction

Curcumin is a natural yellow pigment isolated from the rhizomes of *Curcuma longa* and is broadly used as an additive in food. Curcumin has been used for several centuries in herbal medicines in India, China, and Asian countries. Curcumin has attracted much attention due to its various medicinal properties against expanding and dangerous diseases, such as different types of cancer, and diabetes.<sup>1</sup> Various biological activities, including antioxidant,<sup>2</sup> anti-inflammatory,<sup>3</sup> antiviral,<sup>4</sup> antibacterial,<sup>5</sup> neuroprotective,<sup>6</sup> antifungal,<sup>7</sup> wound healing,<sup>8</sup> and many more have been reported for curcumin. Also, it has been found that curcumin shows pharmacological activity against many human diseases, including multiple sclerosis, rheumatoid

arthritis, Parkinson's and Alzheimer's disease, and atherosclerosis.<sup>9-11</sup>

Despite all the outstanding properties of curcumin, this molecule has insignificant absorption and bioavailability due to limitations such as rapid metabolism, and low water solubility and stability. Many researchers have tried to overcome these problems by modifying the structure, synthesizing the different derivatives and designing the smart drug delivery systems. The chemical structure of curcumin and its active groups is shown in Fig. 1. From the synthetic point of view, there are four active sites in the structure of curcumin for use in the synthesis of new curcumin derivatives. Many researchers have chosen the hydroxyl group to modify the curcumin structure.<sup>12,13</sup> Nucleophilic addition to the enone moiety is another way to synthesize new derivatives.<sup>14,15</sup> The methylene group is an active site that causes the rapid metabolism of curcumin and removes it from the body. Hence, the modification of curcumin through the condensation reaction on the methylene site has attracted a lot

Department of Chemistry, Faculty of Science, Lorestan University, Khorramabad, Iran.  
 E-mail: [sakineh.omidi@yahoo.com](mailto:sakineh.omidi@yahoo.com); Tel: +98-9181438542



*Sakineh Omidi obtained her MS and PhD degrees in Organic Chemistry from Lorestan University, Iran in 2012 and 2018, respectively. This was followed by postdoctoral work with Professor Ali Kakanejadifard at the University of Lorestan. Her current research focuses on the development of biocompatible nanoformulation of curcumin for various biological applications.*



*Ali Kakanejadifard was born in Khorramabad, Iran, in 1957. He studied Organic Chemistry at the University of Tehran, where he obtained his MS degree in 1990 and PhD in 1997 under the guidance of Prof. Morteza Farinia. In 2008 he was appointed Full Professor of Organic Chemistry at the Lorestan University in Khorramabad. His main research interests are in organic synthesis including synthesis and complexation of Schiff bases, di-oximes and azo-azomethine. His work is documented in over 115 scientific papers, and 2 books.*



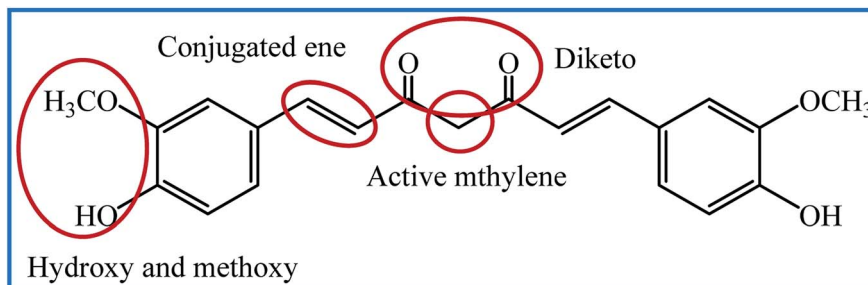


Fig. 1 The active groups of curcumin.

of attention.<sup>16,17</sup> Curcumin is a rare example of naturally ligands having the  $\beta$ -diketone group. This group can contribute to condensation reactions, including Schiff base reaction. Although several review articles have been published on medicinal and biological activities of curcumin analogues,<sup>18–22</sup> to the best of our knowledge, Schiff base, hydrazone, and oxime analogues of curcumin have not been reviewed. In this review, we provide an account of the synthesized curcumin-based derivatives using Schiff base reaction on the  $\beta$ -diketone group, which results in the formation of Schiff base, hydrazone, oxime, and some oxime ether compounds. The most detailed discussion will be focused on the medicinal and biological information of these compounds.

## 2. Schiff base derivatives of curcumin

### 2.1. Schiff bases

The reaction between the substances containing amino groups ( $\text{NH}_2$ ,  $\text{NH}_2\text{OH}$ ,  $\text{NH}_2\text{--NH}_2$ , etc.) with carbonyl groups (aldehydes or some ketones) in honor of the German chemist, Hugo Schiff, is called the Schiff base reaction. In 2011, Kulandaishamy reported the synthesis of tetradeятate chelate **1** and its  $\text{Cu}(\text{II})$ ,  $\text{Ni}(\text{II})$ ,  $\text{Co}(\text{II})$ ,  $\text{VO}(\text{II})$ , and  $\text{Zn}(\text{II})$  complexes (Fig. 2). The antibacterial and antifungal activities of the ligand and their complexes were evaluated against *Escherichia coli* (*E. coli*), *Salmonella typhimurium* (*S. typhi*), *Staphylococcus aureus* (*S. aureus*), *Streptococci*, and *Pseudomonas aeruginosa* (*P. aeruginosa*) bacteria and *Candida albicans* (*C. albicans*) fungi by disc diffusion method. All the metal complexes showed better biological properties than the free ligand, and  $\text{Zn}(\text{II})$  complex exhibited the highest antimicrobial activity (Zone of inhibition in mm: 9–14).<sup>23</sup>

The Knoevenagel condensation can lock the curcumin in the keto tautomer, which leads to an effective reaction with amines to form the Schiff bases. With this strategy, Tharmaraj and co-workers synthesized a non-enolizable diketone of curcumin by indole-3-aldehyde. The reaction of curcumin diketimine and 2,4-diamino-6-phenyl-1,3,5-triazine formed the Schiff base **2**. The synthesis process was followed with forming the metal(II) complexes. The authors evaluated the nonlinear properties and pharmacological activities of compounds. Nonlinear optical (NLO) materials play significant roles in a broad range of photonic applications. Curcumin Schiff base **2** with a conjugated electron structure can have great nonlinear polarizabilities. The compounds were screened against *Streptococcus*

*pyogenes* (*S. pyogenes*) and *S. aureus* bacteria and *Aspergillus flavus* (*A. flavus*) and *Penicillium digitatum* (*P. digitatum*) fungi. All metal(II) complexes showed improved activities compared to compound **2**. The copper complex exhibited higher antibacterial activity (zone of inhibition in mm: 23) than the amikacin (zone of inhibition in mm: 18) against *S. aureus*.<sup>24</sup>

In 2014, Haneefa *et al.* synthesized a Schiff base ligand by a simple condensation of curcumin and aniline with improved biological activities compared the curcumin.<sup>25</sup> Later, they utilized the obtained curcumin-aniline to functionalization of copper oxide nanoparticles in a green synthesis.<sup>26</sup> The bio-functionalized copper oxide nanoparticles indicated potent antimicrobial activity, particularly against *Bacillus subtilis* (*B. subtilis*) (zone of inhibition in mm: 19) and *Aspergillus niger* (*A. niger*) (zone of inhibition in mm: 20) species.

Using tetraaza 14-membered **3**, a series of  $[\text{M}(\text{LL})]^2+$  complexes metals were synthesized and evaluated for interaction with Calf thymus (CT)-DNA using of UV-visible, emission and circular dichroism (CD) spectroscopic methods. This structure can be a mimicking of natural tetraaza macrocycles, such as porphyrins. All complexes showed the interactions with DNA by a groove binding mode and copper complex exhibited a higher degree of interactions with binding constant ( $K_b$ ) =  $1.4 \times 10^5$  (ref. 27). In 2019, a supported catalyst was organized by immobilization of the copper complex **3** on silica gel and used as the catalyst for the synthesis of some tetrazole compounds.<sup>28</sup>

Revathi and co-workers modified the curcumin in methylene and keto (**4** in Fig. 2) groups and evaluated their antioxidant activities using 2,2-diphenyl-1-picrylhydrazyl (DPPH) assay. The obtained Knoevenagel condensates bearing *N,N*-dimethylamino benzaldehyde and 4-hydroxy benzaldehyde were slightly more active than curcumin ( $\text{IC}_{50}$  values about 50  $\mu\text{M}$ ). Substitution on the keto site reduced the antioxidant activity, and  $\text{IC}_{50}$  value for compound **4** was not attained even to 250  $\mu\text{M}$  for compound **4**.<sup>29</sup>

Camp and D'hooghe and co-workers considered the labile  $\beta$ -diketo structure responsible for the low bioavailability of curcumin. Therefore, they synthesized thirteen new derivatives bearing a  $\beta$ -enaminone using the microwave irradiation (**5** in Fig. 2). The antioxidant activities were examined by DPPH and the ferric reducing ability of plasma (FRAP) assays. Compounds **5a–f** exhibited high antioxidant activities by both tests (0.08–0.13% inhibition per  $\mu\text{M}$  by DPPH assay and 0.83–1.29 Trolox equiv. per  $\mu\text{M}$  by FRAP assay) which was comparable to the activity of curcumin (0.15% inhibition per  $\mu\text{M}$  by DPPH assay



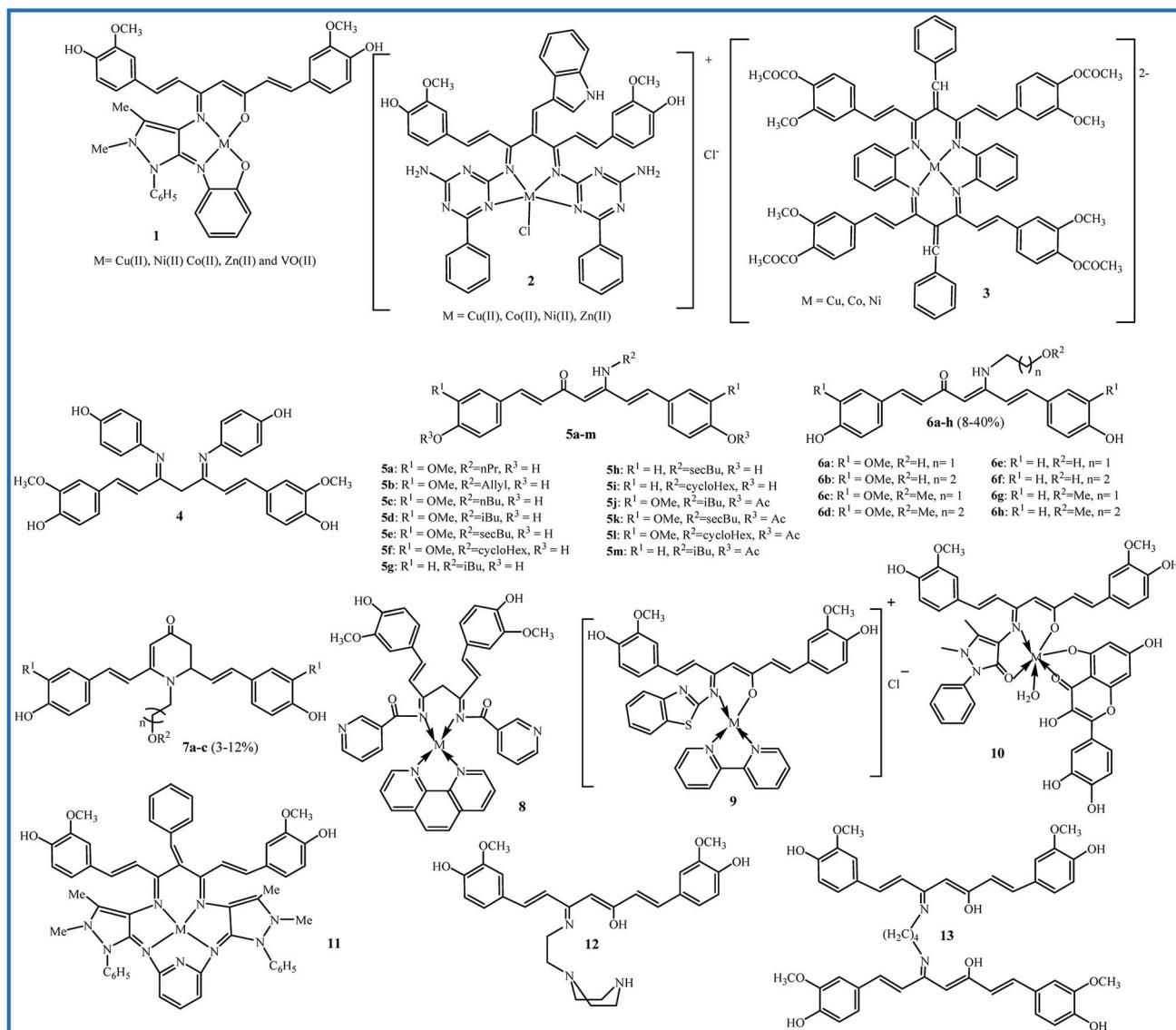


Fig. 2 Structure of Schiff base derivatives of curcumin.

and 1 Trolox equiv. per  $\mu\text{M}$  by FRAP assay). Compounds **5a-f**, like curcumin, contain the  $-\text{OCH}_3$  group in the *ortho* position of the phenol group on the aromatic rings. Compounds without an *ortho* methoxy group (**5g-i**) showed only insignificant antioxidant activities by both assays. For compounds **5j-m** that phenolic groups were protected through acetylation, no antioxidant activity was observed. Cell growth inhibition ( $\text{IC}_{50}$  values in  $\mu\text{M}$ ) of curcumin derivative was evaluated against several cell lines included HT-29, Caco-2 (under undifferentiated and differentiated conditions), EA.hy962, and Chinese hamster ovarian CHO-K1 by determining two parameters of mitochondrial activity and protein content of cells. The results showed that none of the derivatives caused cytotoxic effects on differentiated Caco-2 cells. These cells are similar to *in vivo* enterocytes lining the intestinal tract. It can be concluded that analogues do not disturb the intestinal barrier by cell damage. Also,  $\beta$ -enaminone analogues **5g-i** were cytotoxic for all

undifferentiated cell lines, and **5i** displayed the most significant cytotoxic ( $IC_{50}$  for CHO, Caco-2 undiff, and HT-29 were 9.2, 7.8, and 4.0  $\mu$ M, respectively). Reactive oxygen species (ROS) assay did not show a relationship between ROS induction and decreased cell viability. Therefore, these derivatives did not exert the anticancer properties through ROS induction.<sup>30</sup>

The water solubility of **5a-m** derivatives was similar to curcumin. Therefore, following this work, Camp and D'hooghe research team extended the  $\beta$ -enaminone compound using more polar amines to enhance the water solubility without reducing the biological activity of the obtained curcuminoids. The reaction of the curcumin and hydroxyalkyl amines or methoxyalkyl amines produced eight new  $\beta$ -enaminone analogues (**6a-h**) with extra polar hydroxyl and methoxy groups. Three cyclic dihydropyridinone **7a-c** side-products were also formed in low yields through the suggested mechanism in Fig. 3. The water solubility of **6a-h** and **7a-c** were enhanced 8- to

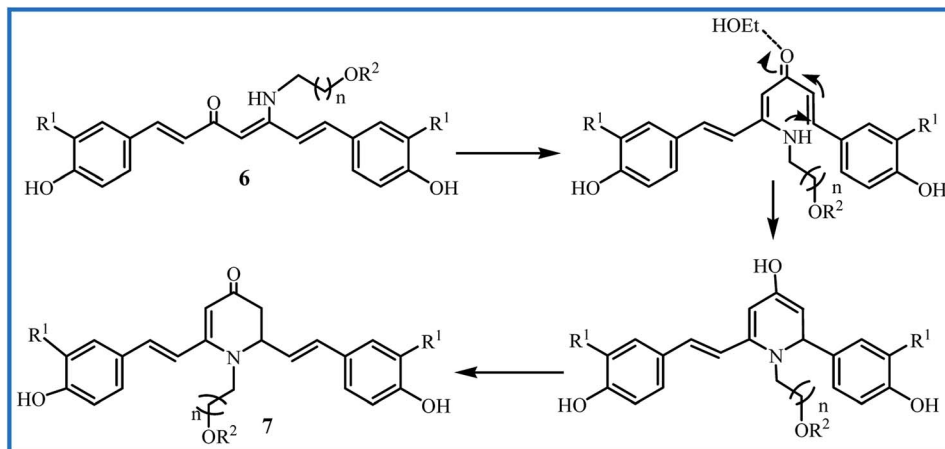


Fig. 3 The suggested mechanism for formation of dihydropyridine-4-ones 7a–c.

37-fold and 16- to 38-fold compared to curcumin, respectively. The new enaminone analogues **6a–d** and **7a** exhibited antioxidant activities comparable to curcumin and much better than bisdemethoxycurcumin derivatives **6e–h** and **7b–c**. In addition, 3-(4,5-dimethylthiazol-2-yl)-2,5-diphenyltetrazolium bromide (MTT) assay showed that cytotoxic activity of **6e–h** ( $IC_{50}$  24–66  $\mu$ M) was better than **6a–d** ( $IC_{50}$  > 54  $\mu$ M) in Caco-2, HepG2, HT-29 and CHO-K1 cells. The cyclic dihydropyridinone **7a–c** did not show notably anti-proliferative activity.<sup>31</sup>

An impressive synthesis of the new curcumin-based ligand has been reported by Abdul Kareem *et al.* They showed that treatment of curcumin and nicotinamide produce a bidentate ligand that can form the Co(II), Ni(II) and Cu(II) complexes with 1,10-phenanthroline compound (**8** in Fig. 2). The highest antibacterial activity against *E. coli*, *S. aureus*, *Klebsiella pneumonia* (*K. pneumonia*), *S. pyogenes* and *P. aeruginosa* were recorded for Cu(II) complexes (bacterial growth inhibition about 80–88%), slightly lower than the standard drug ciprofloxacin (bacterial growth inhibition about 90–98%). The Cu(II) complex also exhibited higher anthelmintic activity against the earthworms *Pheretima posthuma* than other metal complexes (shorter paralysis and mortality times of worms). The authors believed that the more lipophilic nature of the metal atom leads to efficient permeation of the compound through the lipid layer of cell membranes.<sup>32</sup>

In 2017, Raman *et al.* described the synthesis of a Schiff base ligand having 2-aminobenzothizole moiety and its metal complexes by 2,2'-bipyridine as co-ligand (**9** in Fig. 2). Absorption spectral titration experiments showed that complexes have a significant binding affinity with CT DNA ( $K_b$  values  $1.1\text{--}4.3 \times 10^4 \text{ M}^{-1}$ ). DNA cleavage study using pBR322 circular plasmid DNA in the presence of oxidant  $\text{H}_2\text{O}_2$  showed that all complexes are the most potent nucleases. The oxidative damage to DNA over the formation of active oxygen species may result from the oxidation of metal ion from +2 to +3 through Fenton-type reactions. The antibacterial test against *S. aureus*, *B. subtilis*, *E. coli*, *P. aeruginosa* and *S. typhi* showed MIC values  $8.1\text{--}14.4 \times 10^4 \text{ }\mu\text{M}$ . The antifungal test against *A. niger*, *Fusarium solani* (*F. solani*), *Curvularia lunata* (*C. lunata*), *Rhizoctonia bataticola* (*R. bataticola*),

and *C. albicans* showed MIC values  $8.4\text{--}14.8 \times 10^4 \text{ }\mu\text{M}$ . The most significant activities were observed for copper complex due to its high polarizing nature and lipophilicity.<sup>33</sup> In the same year, Raman reported another Schiff base ligand having 4-aminoantipyrine moiety and its metal complexes by quercetin as co-ligand (**10** in Fig. 2). Interactions of these metal complexes with DNA ( $K_b = 1.2\text{--}2.75 \times 10^4 \text{ M}^{-1}$ ) were slightly weaker than complexes of ligand **9**. MIC values of antibacterial and antifungal activities of complexes against the same microbes were about  $4.0\text{--}6.8 \times 10^4 \text{ }\mu\text{M}$  and  $12.1\text{--}17.5 \times 10^4 \text{ }\mu\text{M}$ , respectively that indicated complexes of **10** are potent antibacterial agents.<sup>34</sup>

The evaluation of antibacterial and antifungal activities of 14-membered macrocyclic pentaza **11** and its Cu(II), Ni(II), Co(II), V(II) and Zn(II) complexes showed that all metal compounds have lower MIC values. The copper and zinc complexes exhibited the most potent antimicrobial activities against *E. coli* and *C. albicans* with MIC values 14 and 21  $\text{mg L}^{-1}$ . The antibacterial activity of the vanadium complex did not show notable differences with the free ligand. The copper complex was also showed higher cytotoxicity against breast cancer cell line MCF-7 ( $IC_{50}$  value 47.98  $\mu\text{M}$ ) compared to ligand **11** ( $IC_{50}$  value 75.70  $\mu\text{M}$ ).<sup>35</sup>

In 2018, Schiff base ligand containing ethylene piperazine **12** and their Co(II), Ni(II), Cu(II) and Zn(II) complexes was reported and studied for their antioxidant activity by DPPH assay and cytotoxic potential against MDA-MB-231, KCL22 and HeLa human cancer cell lines by MTT assay. The most significant antioxidant activity was observed for copper and zinc complexes with % scavenging activity  $41.2 \pm 1.75$  and  $40.5 \pm 1.39$  at 15  $\mu\text{M}$  concentrations. The highest cytotoxicity was also observed for copper complex against MDA-MB-231 and KCL22 cells ( $IC_{50}$  values of  $9.13 \pm 1.18$  and  $9.87 \pm 1.95 \mu\text{M}$ ) and zinc complex against HeLa cells ( $IC_{50}$  value of  $12.19 \pm 1.52 \mu\text{M}$ ). All metal complexes revealed the enhancement in the biological activities compared to the free ligand. It can be attributed to the existence of azomethine bond in the chelate ring and lipophilic nature of the metal ions, which improve their penetration *via* the lipid layer of the cell membrane.<sup>36</sup>

Recently, a new Schiff base of curcumin (**13** in Fig. 2) was synthesized and used as a self-stabilizing and reducing agent in

green synthesis of silver nanoparticles in water due to its high-solubility in aqueous solutions. Compared to curcumin, compound **13** exhibited higher activity against Gram-negative bacteria (*E. coli* and *P. aeruginosa*) and lower activity against Gram-positive bacteria (*S. aureus* and *B. subtilis*).<sup>37</sup>

The synthetic methodology, yields, and distinct biological activity of **1–13** are summarized in Table 1.

## 2.2. Schiff base derivatives with other functional groups

**2.2.1 Sulfonamides.** Sulfonamides are important pharmacores which are widely employed in new drug designing. In this

regard, two series of Schiff base-curcumin including sulfonamide moiety **14a–e** and **15a–e** (Fig. 4) were synthesized by Lal *et al.* For these compounds, antibacterial activity against *S. aureus*, *Bacillus cereus* (*B. cereus*), *S. typhi*, *P. aeruginosa*, and *E. coli*, and antifungal activity against *A. niger*, *A. flavus*, *C. lunata*, and *Trichoderma viride* (*T. viride*), were screened. The cytotoxic activity of compounds tested by HeLa, Hep-G2, QG-56 and HCT-116 cancer cell lines. The *in vivo* anti-inflammatory activity evaluated using the carrageenan-induced paw oedema method. The bioassay results approved that the activity of sulfonamides can be further improved when coupled with curcumin.

Table 1 Summary of properties of compounds **1** to **13**

Compound	Condition of synthesis	Yield (%)	Activity	Outcome	Reference
<b>1</b>	6 h reflux of precursors in EtOH	80	Antibacterial	Zn(II) complex showed the highest activity but was not compared with curcumin	23
<b>2</b>	6 h stirrer of precursors in EtOH at room temperature and in presence of piperidine	72	Antibacterial and antifungal	Cu(II) complex showed the highest activities but was not compared with curcumin	24
<b>3</b>	24 h reflux of precursors in MeOH	No reported	DNA cleavage	Cu(II) complex showed the highest $K_b$	28
<b>4</b>	6 h stirrer of precursors in MeOH at room temperature and in presence of piperidine	56.9	Antioxidant	Lower antioxidant activity compared to curcumin	29
<b>5a–i</b>	Heating of precursors in 2-methyl-THF or $\text{CHCl}_3$ under microwave irradiation for 1–1.75 h at 80 °C in presence of MK10 clay and acetic acid	11–58	Anticancer and antioxidant	<b>5a–f</b> showed comparable antioxidant activity to curcumin, <b>5i</b> was strongest anticancer agent	30
<b>5j–m</b>	Heating of <b>5d–g</b> and acetic anhydride in 2-methyl-THF in presence of pyridine	42–67	Anticancer and antioxidant	No antioxidant activity and low anticancer activity	30
<b>6a–h</b>	Heating of precursors in 2-methyl-THF or EtOH or DMF under microwave irradiation for 1–1.5 h at 70–100 °C in presence of MK10 clay and acetic acid	8–40	Anticancer and antioxidant	Enhanced water-solubility and anticancer activity and comparable antioxidant activity ( <b>6a–d</b> ) to curcumin	31
<b>7a–c</b>	Heating of precursors in EtOH under microwave irradiation for 1–1.5 h at 70–100 °C in presence of MK10 clay and acetic acid	3–12	Anticancer and antioxidant	Enhanced water-solubility compared to curcumin	31
<b>8</b>	12 h reflux of precursors in MeOH	74	Antibacterial and anthelmintic	Cu(II) complex showed the highest activities but was not compared with curcumin	32
<b>9</b>	4 h reflux of precursors in EtOH	66	Antibacterial/antifungal and DNA cleavage	Cu(II) complex showed the highest activities but was not compared with curcumin	33
<b>10</b>	3 h reflux of precursors in EtOH	75	Antibacterial/antifungal and DNA cleavage	Cu(II) complex showed the highest activities but was not compared with curcumin	34
<b>11</b>	24 h reflux of precursors in EtOH in presence of anhydrous $\text{K}_2\text{CO}_3$	No reported	Antibacterial/antifungal and anticancer	Cu(II) complex showed the highest activities but was not compared with curcumin	35
<b>12</b>	6 h reflux of precursors in MeOH	74	Anticancer and antioxidant	Cu(II) and Zn(II) complexes showed the highest activities but was not compared with curcumin	36
<b>13</b>	6 h reflux of precursors in EtOH in presence of acetic acid	85	Antibacterial	Higher activity against Gram-positive and lower activity against Gram-negative bacteria compared to curcumin	37



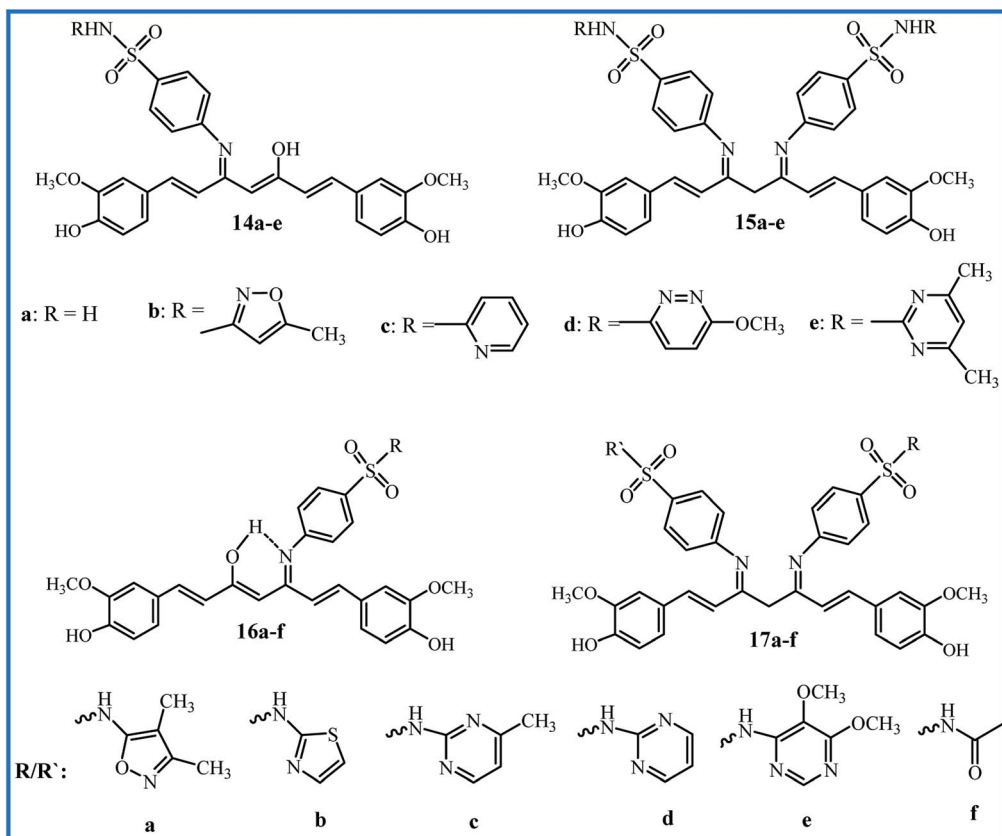


Fig. 4 Sulfonamide derivatives of curcumin.

Compounds **14a–e** containing one sulfonamide molecule showed the higher antibacterial and antifungal activities than compounds **15a–e** with two sulfonamide molecules attaching on both carbonyls of curcumin. Compounds **14b–e** (MIC 20  $\mu$ M against all bacteria) and **14e** (MIC 20  $\mu$ M against all fungi, except *A. flavus*) were more active. The cytotoxic experiments confirmed that compounds **14b–e** ( $IC_{50}$  values 25–50  $\mu$ M) were more cytotoxic as comparative to curcumin ( $IC_{50}$  values 50–100  $\mu$ M). Among compounds **15a–e**, only **15e** ( $IC_{50}$  values 25–50  $\mu$ M) exhibited higher cytotoxicity than curcumin. Also, compounds **15e** and **14e** exhibited the highest anti-inflammatory activity, with percentage inhibition of 40.3 and 38.7, respectively. Generally, the results of this study purposed that the enolic group required for biological activities.<sup>38</sup>

Ahmed *et al.* reported the synthesis of a series of curcumin-Schiff bases bearing one or two benzenes sulfonamides moieties (**16a–f** and **17a–f** in Fig. 4). The compounds were investigated for antibacterial activity against *Salmonella enterica* (*S. enterica*), *E. coli*, *P. aeruginosa*, *K. pneumonia*, *S. aureus*, and Methicillin-resistant *S. aureus* (MRSA) bacteria, antifungal activity against *A. niger*, *A. flavus*, *F. solani*, *Fusarium oxysporum* (*F. oxysporum*), *Alternaria alternate* (*A. alternate*) and *P. digitatum* fungi, anti-inflammatory activity (using carrageenan-induced hind paw edema technique), and anti-nociceptive activity (by acetic acid-induced method). Compound **16a** with isoxazole moiety was the most potent compound in anti-inflammatory (%

inhibition 82.0), anti-nociceptive (% inhibition 66.8), and anti-bacterial (MIC 15.63–31.25  $\mu$ g mL<sup>−1</sup>) activities; compound **16b** with 4-methylpyrimidin moiety exhibited the highest antifungal activity (MIC 31.25–125  $\mu$ g mL<sup>−1</sup>) against *F. solani*, *F. oxysporum*, and *A. alternate*. Furthermore, the combinations of **16a** with standard antibacterial drug ciprofloxacin or standard anti-fungal drug nystatin indicated the notable synergic effects. The combination of ciprofloxacin (0.12  $\mu$ g mL<sup>−1</sup>) with compound **16a** (7.8  $\mu$ g mL<sup>−1</sup>) was 8-fold more potent than ciprofloxacin, and inhibited the growth of MRSA.<sup>39</sup> This research group also conducted *in vitro* urease inhibition studies, and indicated these compounds are moderate to good urease enzyme inhibitors.<sup>40</sup>

The synthetic methodology, yields, and distinct biological activity of **14–17** are summarized in Table 2.

**2.2.2 Amino acids.** Amino acids are including both amine and carboxylic functional groups, and play an important role in physiological functions. The amino group can perform the Schiff base reaction with molecules containing  $\beta$ -diketones such as curcumin. In 2013, Raman's team, in the search for selective anticancer agents, synthesized the Schiff base ligand **18** (Fig. 5) by condensation of curcumin and cysteine  $\alpha$ -amino acid.<sup>41</sup> The oxygen and nitrogen of ligand were coordinated to Cu(II), Co(II), Ni(II), and Zn(II) metal ions. The interaction of the ligand **18** and its complexes with DNA is evaluated. The electronic absorption spectra showed that there is a strong

Table 2 Summary of properties of compounds 14 to 17

Compound	Condition of synthesis	Yield (%)	Activity	Outcome	Reference
<b>14a–e</b>	3–4 h reflux of precursors in EtOH	87–91	Antibacterial/antifungal and anti-inflammatory	<b>14b–e</b> showed higher activity compared to curcumin	38
<b>15a–e</b>	2–3 h heating of precursors in EtOH at 60 °C in presence of acetic acid	91–94	Antibacterial/antifungal and anti-inflammatory	Only <b>15e</b> showed higher activity compared to curcumin	38
<b>16a–f</b> and <b>17a–f</b>	Reflux of precursors in EtOH in presence of acetic acid	71.5–92.5	Antibacterial/antifungal and anti-inflammatory	<b>16a</b> was most potent compound	39

interaction between the complexes and DNA bases ( $K_b = 1.2\text{--}3.4 \times 10^4 \text{ M}^{-1}$ ), which could cause DNA-cleavage. Using pBR322 circular plasmid DNA, gel electrophoresis experiments were carried out in the presence of  $\text{H}_2\text{O}_2$  as an oxidant. It was revealed that all the complexes are efficient cleaving agents. Also, the results of the antibacterial assay against *S. aureus*, *B. subtilis*, *E. coli*, *P. aeruginosa*, and *S. typhi* bacteria and anti-fungal assay against *A. niger*, *F. solani*, *C. lunata*, *R. bataticola*, and *C. albicans* strains showed that the complexes (MIC = 11.2–15.0 and 12.1–15.9  $\mu\text{g mL}^{-1}$  for antibacterial and antifungal, respectively) exhibited better activity than the ligand (MIC = 17.3–19.5 and 18.1–19.3  $\mu\text{g mL}^{-1}$  for antibacterial and anti-fungal activities, respectively). In a later investigation, this research team prepared a Knoevenagel condensed by the reaction of curcumin and *p*-nitro benzaldehyde. They then synthesized the Schiff base ligand **19** by methionine amino acid. The metal complexes of **19** showed a higher interaction with DNA ( $K_b = 2.0\text{--}4.7 \times 10^4 \text{ M}^{-1}$ ) compared to the complexes of compound **18**. Also, all complexes displayed significant toxicity against above bacteria (MIC = 9.3–14.1  $\mu\text{g mL}^{-1}$ ) and fungi (MIC = 8.6–15.9  $\mu\text{g mL}^{-1}$ ). The copper complex was the most potent compound due to the increase in the size of the metal ion and the decrease in the polarization, which leads to an increase in the lipophilic character.<sup>42</sup> In another study, Raman's team reported the synthesis of a tridentate metal(II) chelates (**20** in Fig. 5) and its metal(II) complexes by reaction of L-tryptophan and a Knoevenagel condensed of curcumin. The complexes of **20** exhibited the lower interaction with DNA ( $K_b = 1.8\text{--}3.4 \times 10^4 \text{ M}^{-1}$ ), lower antibacterial and antifungal activities (MIC: 9.8–15.7 and 9.6–15.9  $\mu\text{g mL}^{-1}$ , respectively) compared to

complexes of compound **19**. This study furthermore showed that complexes strongly bound through an intercalation mechanism with the DNA. These compounds were potent DNA cleaving agents in the presence of  $\text{H}_2\text{O}_2$ .<sup>43</sup>

The synthetic methodology, yields, and distinct biological activity of **18–20** are summarized in Table 3.

### 2.3. Schiff base derivatives of curcumin's analogues

Improving the bioavailability and stability of curcumin can be one of the goals to form the new analogues of curcumin. Recently, Camp, D'hooghe and co-workers focused on a class of aza-aromatic curcuminoids, including pyridine-, indole-, and pyrrole-based curcumin analogues with slightly improved water solubility compared to the curcumin. Subsequently, they selected the bispyridine analogue to be used in the Schiff base reaction and preparation of the corresponding  $\beta$ -enaminone derivatives (**21a-f** and **22d,f** in Fig. 6). It was founded that  $\beta$ -enaminone **21a-f** and **22d,f** (bearing a polar aliphatic moiety) indicated remarkably increase in water solubility in the range of 4 to 1600-fold compared to curcumin. The evaluation of anti-oxidant activities using DPPH and FRAP assays indicated a decrease compared to curcumin, which can be attributed to the absence of hydroxyl groups in the aromatic rings of these compounds. The evaluation of cytotoxic effects of compounds by MTT assay and cancer cell lines HepG2, EA.hy926, Caco-2, HT-29, and CHO-K1 demonstrated that **21a-d** exhibited moderate growth inhibition, while **21e** and **21f** indicated no activity at concentration 75  $\mu$ M. The  $\beta$ -enaminone **21a** exhibited the highest anti-proliferative activity that was similar to the

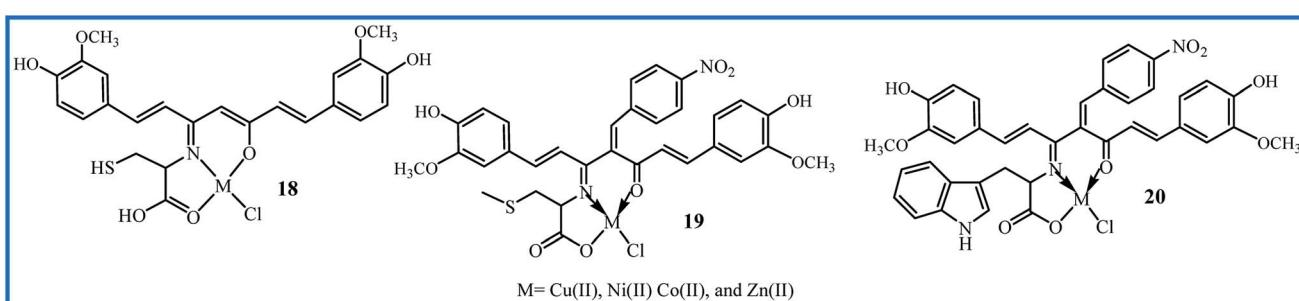


Fig. 5 Structure of amino acid derivatives of curcumin.

Table 3 Summary of properties of compounds 18 to 20

Compound	Condition of synthesis	Yield (%)	Activity	Outcome	Reference
18	6 h reflux of precursors in EtOH	60	Antibacterial/antifungal and DNA cleavage	Cu(n) complex showed the highest activities but was not compared with curcumin	41
19	6 h reflux of precursors in EtOH	60	Antibacterial/antifungal and DNA cleavage	Cu(n) complex was the most potent compound but was not compared with curcumin	42
20	6 h reflux of precursors in EtOH	63	Antibacterial/antifungal and DNA cleavage	Cu(n) complex showed the highest activities but was not compared with curcumin	43

activity of curcumin. Intracellular ROS for compounds was dependent on the cell types. Compounds 21a–e indicated moderate to high ROS generation at 10  $\mu$ M only in Caco-2 cells. In general, *N*-alkyl  $\beta$ -enaminone curcuminoids presented an acceptable balance between good water solubility and notable bioactivity. The authors proposed that  $\beta$ -enaminone curcuminoids with nonpolar aliphatic side chains can be used for further progress in medicinal chemistry.<sup>44</sup>

Recently, Mahal and co-workers used the tetrahydrocurcumin (THC), a metabolite of curcumin, to prepare thirteen Schiff base derivatives 23a–m.<sup>45</sup> All compounds showed moderate to good anti-cancer activity against cancer cell lines A549, HeLa and MCF-7, except compounds 23a and 23m ( $IC_{50} > 50 \mu$ M). Compound 23l with a  $CF_3$  group at the *para*-position of the phenyl ring showed the highest activity ( $IC_{50}$  values 4.8  $\mu$ M

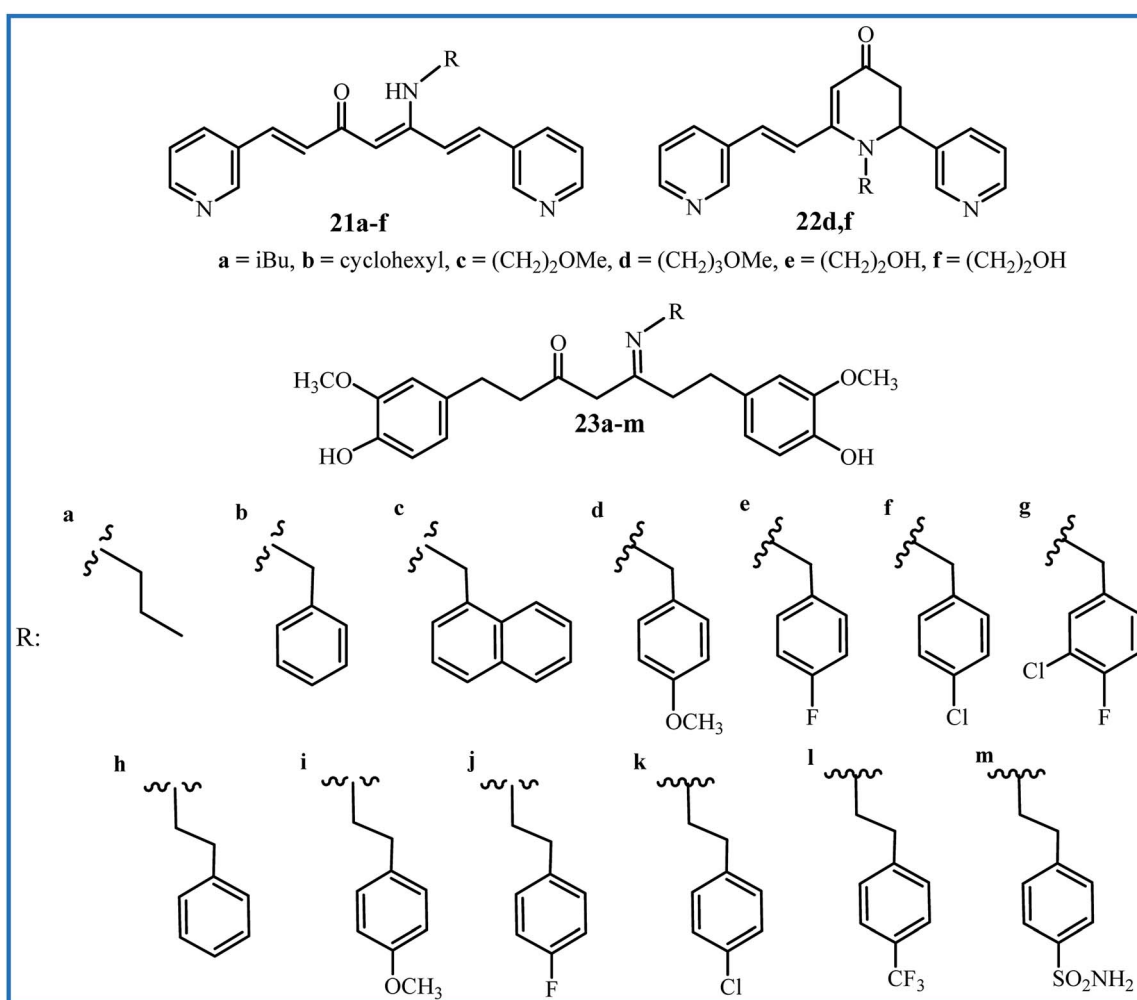


Fig. 6 Structure of Schiff base derivatives of curcumin's analogues.



Table 4 Summary of properties of compounds 21 to 23

Compound	Condition of synthesis	Yield (%)	Activity	Outcome	Reference
21a-f and 22d,f	Heating of precursors in 2-methyl-THF or EtOH under microwave irradiation for 75–105 min at 80–85 °C in presence of MK10 clay and acetic acid	6–24	Anticancer and antioxidant	Enhanced water-solubility, comparable anticancer and lower antioxidant activities to curcumin	44
23a-m	10 h reflux of precursors in EtOH in presence of acetic acid	45–94	Anticancer	23l was the most potent compound but was not compared with curcumin	45

against MCF-7, 11.9  $\mu$ M against A549 and 12.7  $\mu$ M against HeLa cell lines).

The synthetic methodology, yields, and distinct biological activity of 21–23 are summarized in Table 4.

#### 2.4. Schiff base macro-structures for release of curcumin

The use of triggered carrier can improve the circulation-stability and bioavailability of curcumin. One of the interesting syntheses of Schiff base compounds from curcumin has been reported by Riela *et al.* They functionalized the halloysite nanotubes (HNTs) with curcumin through Schiff base formation as a stimuli-responsive linkage. The resulting HNT-curcumin 24 prodrug has dual stimuli-responsive ability upon contact to the glutathione-rich or acidic environment due to the presence of disulfide and imine linkages (Fig. 7a). The anti-proliferative *in vitro* studies against HA22T/VGH and Hep3B cell lines indicated that HNT-Cur prodrug induced high cytotoxicity (% viability < 20 with a curcumin concentration up to 50  $\mu$ M) compared to the free curcumin or pristine HNT (% viability

> 90). The prodrug preserved its antioxidant characteristics and showed excellent stability in normal physiological conditions.<sup>46</sup>

In 2017, Jayakumar and co-workers, during the four-step reactions from  $\gamma$ -polyglutamic acid ( $\gamma$ -PGA), 3-mercaptopropionic acid (3-MPA), and adipic acid dihydrazide (ADH) prepared the ( $\gamma$ -PGA-SS-ADH) polymer. This polymer was conjugated with curcumin *via* hydrazone to obtain  $\gamma$ -PGA-SS-ADH-Cur (25 in Fig. 7b). In the presence of the stabilized aqueous medium, polymeric conjugate 25 was formulated into self-assembled core-shell nanoparticles (NPs) that showed pH and redox-responsive curcumin delivery. The microscopic study of the uptake of NPs by HT-29 cells revealed the presence of NPs in the lysosomes *via* the endocytosis mechanism. NPs exhibited higher cytotoxicity against HT-29 cells at lower pH and the absence of  $H_2O_2$ , which confirms that conjugated 25 can be used as a developing drug delivery system in cancer therapy.<sup>47</sup>

Sathianarayanan *et al.* synthesized the curcumin conjugated chitosan microspheres (CCCMs) by Schiff base reaction between amino groups of chitosan biopolymer and carbonyl groups of curcumin. CCCMs showed the sustained release of

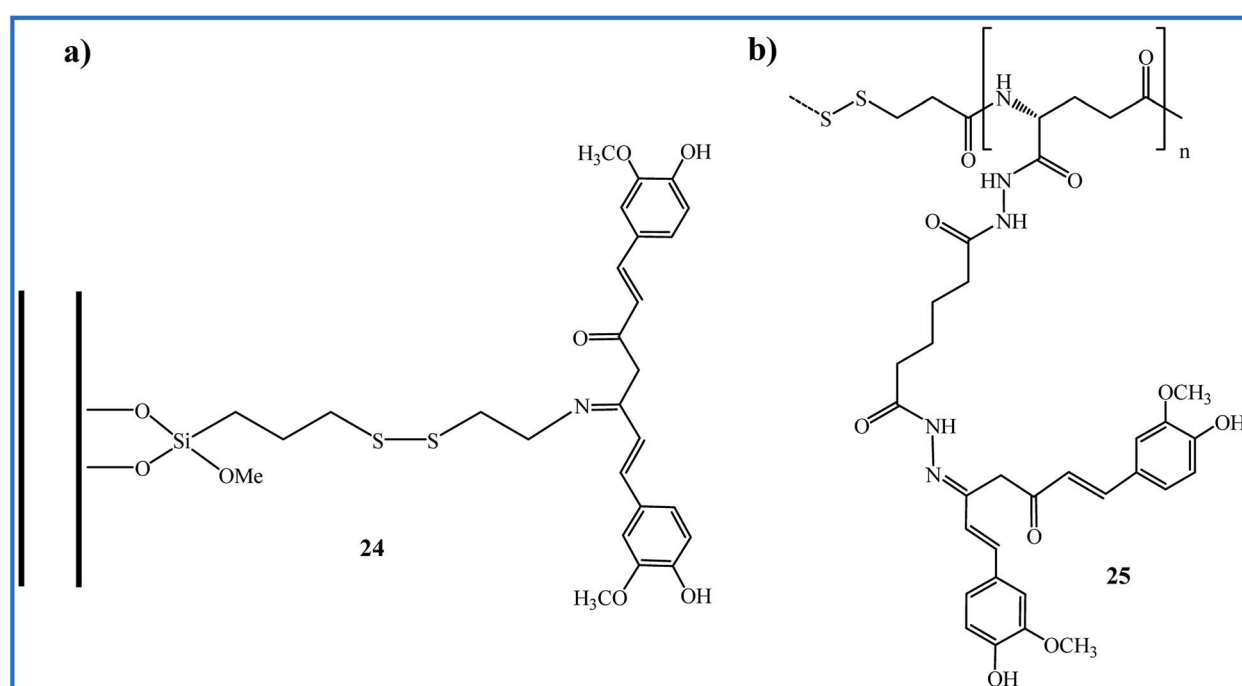
Fig. 7 (a) HNT–Curcumin prodrug, (b) dual responsive  $\gamma$ -PGA-SS-ADH-Cur conjugates.

Table 5 Summary of properties of compounds 24 and 25

Compound	Condition of synthesis	Curcumin loading (wt%)	Activity	Outcome	Reference
24	Stirring of precursors in EtOH under microwave irradiation for 1 h at 80 °C	2.9	Anticancer	The prodrug showed the higher cytotoxicity compared to curcumin	46
25	Stirring of precursors in MeOH/H <sub>2</sub> O for 72 h at 37 °C in presence of acetic acid	5 ± 2	Anticancer	Compound showed a pH and redox-responsive and higher cytotoxicity compared to curcumin	47

curcumin and maximum release observed after 48 h. Antimicrobial activity of CCCMs against *S. aureus* and *E. coli* was relatively higher compared to free curcumin. The results of DPPH and H<sub>2</sub>O<sub>2</sub> assays showed the IC<sub>50</sub> values of 216 µg mL<sup>-1</sup> and 228 µg mL<sup>-1</sup> for CCCMs, respectively, which indicated the antioxidant activity of CCCMs is more or less equal to the free curcumin. The anti-inflammatory potential of CCCMs, obtained by the bovine serum albumin method, was similar to that of curcumin with IC<sub>50</sub> about 45 µg mL<sup>-1</sup>. The prepared microspheres did not exhibit any toxicity in normal NIH 3T3 (mouse embryonic fibroblast) cells, suggesting that CCCMs can be useful for biomedical fields.<sup>48</sup>

In 2018, a delivery nanosystem was designed with the folate (FA)-receptor targeting mesoporous silica nanoparticles to load the curcumin through Schiff base reaction. This designed curcumin-loaded nanoparticles showed higher cellular uptake in FA-receptor-rich MCF-7 cells compared to FA-receptor-poor HEK-293T cell lines. They did not show remarkable toxicity even while the incubated concentration increased to 640 µg mL<sup>-1</sup>.<sup>49</sup>

The synthetic methodology, curcumin loading (wt%), and distinct biological activity of 24 and 25 are summarized in Table 5.

### 3. Hydrazone derivatives of curcumin

Hydrazines (compounds with NH<sub>2</sub>-NH<sub>2</sub> functional group) can easily contribute to Schiff base reaction and form the hydrazone compounds. Venkatesh *et al.* synthesized the curcumin derivative 26 (Fig. 8) by the condensation reaction of curcumin and hydrazine hydrate in a methanol solution. Schiff base ligand 27 was then obtained by further condensation of derivative 26 with methyl salicylaldehyde. The metal chloride salts were used to obtain the Cu(II), Ni(II), and Zn(II) complexes of ligand 27. This study was useful to considerate the interaction mechanism of the complexes with DNA, and it can be valuable in the new chemotherapy drug progress. The *in vitro* DNA binding studies were performed by the absorption titration of metal complexes with CT-DNA concentrations. The spectroscopic changes indicated the intrinsic binding constants 4.72 × 10<sup>4</sup> M<sup>-1</sup>, 3.89 × 10<sup>4</sup> M<sup>-1</sup>, and 3.13 × 10<sup>4</sup> M<sup>-1</sup> for Cu(II), Ni(II), and Zn(II) complexes, respectively. Fluorescence measurements showed a strong quenching in the emission spectrum of DNA-EB by the addition of metal complexes, which proved the binding of complexes to DNA (EB is a molecular fluorophore that emits

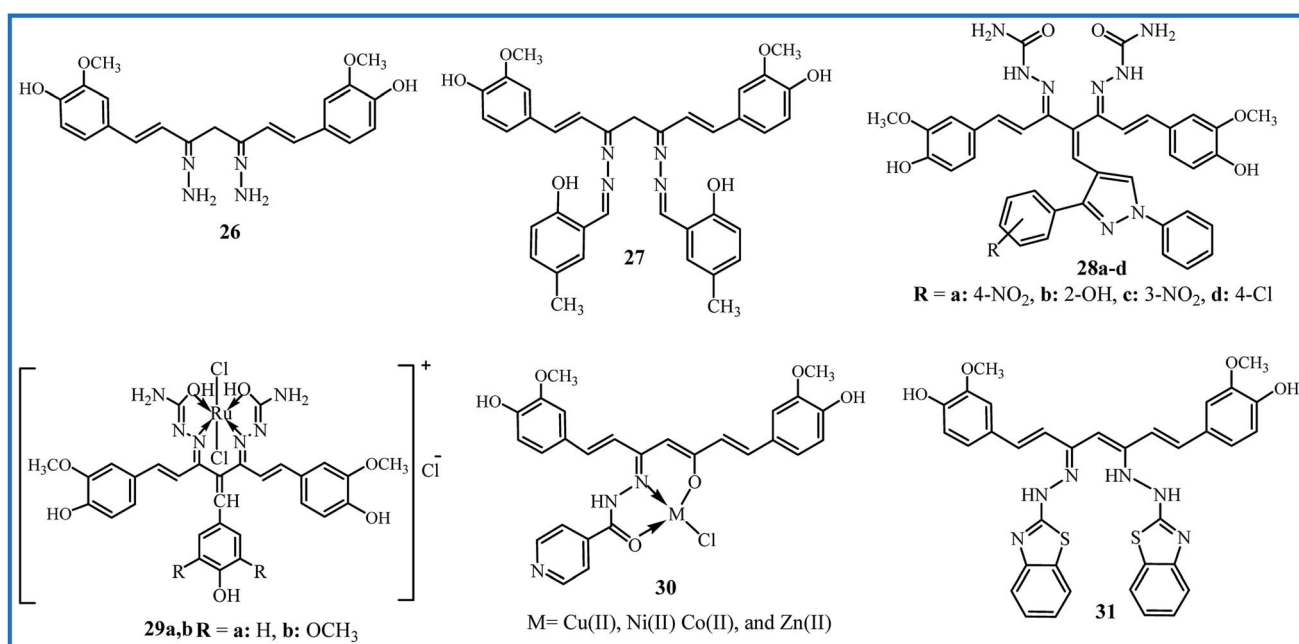


Fig. 8 Structure of hydrazone derivatives of curcumin.





Table 6 Summary of properties of compounds 26 to 31

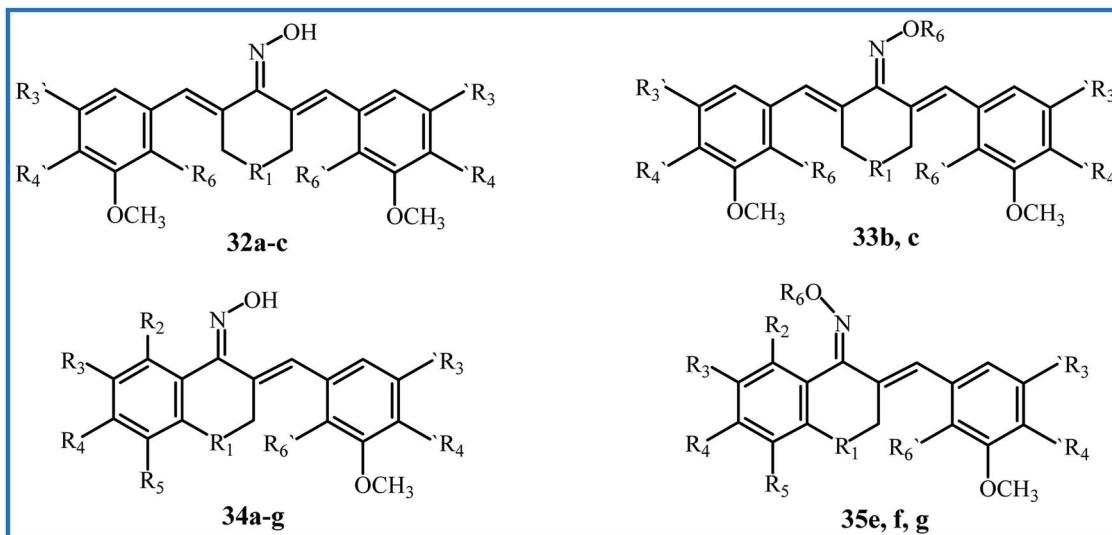
Compound	Condition of synthesis	Yield (%)	Activity	Outcome	Reference
26 and 27	Stirring of precursors in MeOH for 6 h, then 8 h reflux	No reported	DNA cleavage	Cu(II) complex showed the highest $K_b$	50
28a-d	24 h reflux of precursors in $\text{CHCl}_3/\text{MeOH}$ in presence of piperidine	60-67	DNA cleavage and anticancer	All compounds showed the good DNA interacting tendency	51
29	Stirring of precursors in MeOH for 24 h in presence of piperidine	No reported	DNA cleavage and anticancer	Two ruthenium(II) complexes were potent for treatment of cervical cancer	52
30	Reflux of precursors in EtOH for 4 h in presence of acetic acid	80	Antibacterial/antifungal and DNA cleavage	Cu(II) complex showed the highest activities	53
31	Reflux of precursors in EtOH	No reported	Antioxidant	All Cu(II) complexes showed the higher activity than curcumin	54

fluorescence in the presence of CT-DNA). These results revealed that all complexes interact with the DNA through intercalating binding mode, and Cu(II) complex showed better binding affinity than Ni(II), and Zn(II) complexes.<sup>50</sup>

In 2013, an enlarged study was performed on the synthesis and pharmacological properties of a series of Knoevenagel condensates and disemicarbazones derivatives of curcumin.<sup>51</sup> The *ortho*, *meta* and *para*-substituted pyrazolealdehydes were synthesized and applied to prepare of Knoevenagel's condensates with curcumin. The final disemicarbazones products 28a-d (Fig. 8) were obtained by reaction of Knoevenagel's condensates and semicarbazide hydrochloride. The cytotoxicity of the compounds was evaluated by *in vitro* hemolytic assay by Mammalian RBCs, and the interaction of compounds with DNA was studied by UV-vis spectroscopy. The compounds 28a-d showed higher  $K_b$  ( $2.6 \times 10^4$  to  $8.1 \times 10^5 \text{ M}^{-1}$ ) compared to initial pyrazolealdehydes ( $1.4 \times 10^3$  to  $7.6 \times 10^4 \text{ M}^{-1}$ ) and Knoevenagel's condensates derivatives ( $1.4 \times 10^4$  to  $7.8 \times 10^5 \text{ M}^{-1}$ ). The less hemolytic than doxorubicin (7% to 25%), the low cell line viability even at low concentration  $1.0 \mu\text{g mL}^{-1}$ , and high DNA binding constant indicated that compounds 28a-d could be good anticancer agents. The *in vitro* anticancer profiles of compounds have determined by MTT assay against human breast cancer cell line MCF-7, and results showed the viabilities 59% to 79% at  $1.0 \text{ L g mL}^{-1}$ . The initial pyrazolealdehydes derivatives showed higher anticancer activities, which can be attributed to the smaller size and ability to pass the membrane.

The incorporation of metals into the structure of ligands and the formation of complexes enhance the biological activity. Imran's research team synthesized two Knoevenagel derivatives, two ligands and finally two ruthenium(II) complexes of curcumin derivatives (29a,b in Fig. 8) with octahedral geometries. Compared to other metal complexes, ruthenium complexes show improved antitumor activity and higher binding capacities to DNA due to octahedral structures.<sup>52</sup> The binding constants, calculated by UV-vis spectroscopy, were  $1.46 \times 10^4$  and  $3.54 \times 10^4 \text{ M}^{-1}$  for 29a and 29b. The fluorometry spectroscopy also showed the strong binding of compounds with DNA. Determination of the toxicity of complexes was performed by hemolytic assays based on the effects of the compound on human RBCs. The complexes showed lower toxicity than the standard anticancer drug letrozole. Also, they indicated good cytotoxicity against cervical cancer (HeLa) cell line ( $\text{IC}_{50}$  values of 0.004 to 20.35 nM) and moderate cytotoxicity against other cell lines, including liver hepatocellular carcinoma, breast cancer, and human colon adenocarcinoma.

In 2019, the biological activities of curcumin-derived hydrazone 30 and its metal complexes were studied as *in silico* and *in vitro*. The UV-vis spectroscopy verified a groove mode of binding between the CT DNA and metal complexes. The Cu(II) complex with  $K_b$  value of  $2.9 \times 10^{-4} \text{ M}$  showed the highest binding efficiency. The agarose gel electrophoresis technique in the presence of oxidant  $\text{H}_2\text{O}_2$  revealed that complexes could cleave pUC 19 (Plasmid University of California) DNA. So, they can be purposed as the potent anticancer agents. DFT analysis using the Gaussian 09 W Program demonstrated that the

Fig. 9 Structure of new synthetic curcumin-like oxime and oxime ether analogues by Qin *et al.*

copper complex has a higher dipole moment, leading to a better interaction with the biological systems. This higher biological availability is experimentally verified by antimicrobial assays. The metal complexes showed MIC between 3.1 and 5.6 ( $\times 10^{-3}$   $\mu\text{M}$ ) against *S. aureus*, *B. subtilis*, *K. pneumonia*, and *E. coli* bacteria, while MIC values for ligand **30** were between 10.3 and 13.0 ( $\times 10^{-3}$   $\mu\text{M}$ ). Also, MIC values were between 11.1 and 15.4 ( $\times 10^{-3}$   $\mu\text{M}$ ) against *A. niger*, *A. flavus*, *C. lunata*, *R. bataticola*, and *C. albicans* fungi for metal complexes. MIC values for the antifungal activity of ligand **30** were between 20.4 and 22.7 ( $\times 10^{-3}$   $\mu\text{M}$ ). The most significant antibacterial and antifungal activities were shown by Cu(II) complex.<sup>53</sup>

Recently, the hydrazone compound **31**, as a tautomeric form, was prepared by reaction of 2-hydrazinobenzothiazole and curcumin in a 2 : 1 molar ratio. The copper(II) coordination complexes in 1 : 1 and 1 : 2 molar ratios were synthesized using the copper chloride, bromide, acetate and nitrate by template method. The antioxidant capacity was evaluated by comparing the activity of compounds with TROLOX as the standard by photo chemiluminescence method. The total antioxidant capacity of ligand **31** (16.88%) revealed to be slightly lower than the capacity of curcumin (17.07%). All copper complexes, with the total antioxidant capacity between 22.34% and 28.70%, were better antioxidant agents than curcumin attributed to redox reactions within the  $\text{Cu}^{2+}/\text{Cu}^+$  couple. The synthesized complexes by copper nitrate that have 2 : 1 metal : ligand molar ratio, exhibited the highest antioxidant capacity.<sup>54</sup>

The synthetic methodology, yields, and distinct biological activity of **26–31** are summarized in Table 6.

#### 4. Oxime and oxime ether derivatives of curcumin

Oximes, an abbreviation of oxy-imine, and oxime ethers are the advantaged groups in chemistry that show a broad range of biological and pharmaceutical activities.<sup>55,56</sup> In this section, we

reviewed the performed efforts to incorporate these groups into the structure of the curcumin or its analogues.

The first oxime analogue of curcumin was synthesized by Dutta *et al.* in 2001 through condensation of curcumin and hydroxylamine hydrochloride. They also prepared the copper complex of the obtained oxime analogue and showed that copper conjugation strangely improved the antioxidant activity of the parent oxime ligand.<sup>57</sup> In 2008, Simoni *et al.* synthesized two dioxime ether analogues of curcumin by *O*-methyl or *O*-benzyl hydroxylamine hydrochloride. The antitumor effects against MCF-7 and multidrug-resistant (MDR) variant MCF-7R cancer cell lines showed that benzyl oxime derivative has a high antitumor activity even against MDR tumors.<sup>58</sup>

Qin *et al.* conducted extensive research on sixty-nine  $\alpha,\beta$ -unsaturated carbonyl-based compounds, oxime and oxime ether analogues in 2016. Fifteen new oxime and oxime ether compounds **32–35** are shown in Fig. 9, Tables 7 and 8. MTT assay by MCF-10A cells showed that all compounds were nontoxic with cell viability of more than 90%. The structure-activity relationship (SAR) of compounds was determined for their anti-proliferative activity against PC-3, HT-29, MCF-7, H-460, A-549, PaCa-2 and Panc-1 cancer cell lines. All oxime analogues **32a–c** and **34a–g** exhibited more inhibition of cancer cells than parent  $\alpha,\beta$ -unsaturated carbonyl-based compounds, and all oxime ether analogues **33b,c** and **35e,f,g** exhibited less inhibition of cancer cells compared to parent oximes. Oxime

Table 7 Structures of new synthetic oxime and oxime ether **32** and **33**

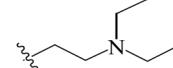
compound	R1	R'3	R'4	R'6	R6
32a	CH <sub>2</sub>	OCH <sub>3</sub>	OCH <sub>3</sub>	Br	
32b, 33b	CH-CH <sub>3</sub>	OCH <sub>3</sub>	OCH <sub>3</sub>	Br	
32c, 33c	N-CH <sub>3</sub>	OCH <sub>3</sub>	OCH <sub>3</sub>	Br	

Table 8 Structures of new synthetic oxime and oxime ether 34 and 35

compound	R <sub>1</sub>	R <sub>2</sub>	R <sub>3</sub>	R <sub>4</sub>	R <sub>5</sub>	R' <sub>3</sub>	R' <sub>4</sub>	R' <sub>6</sub>	R <sub>6</sub>
<b>34a</b>	CH-CH <sub>3</sub>	H	H	H	H	OCH <sub>3</sub>	OCH <sub>3</sub>	Br	
<b>34b</b>	CH <sub>2</sub>	H	H	H	OH	OCH <sub>3</sub>	OCH <sub>3</sub>	Br	
<b>34c</b>	CH <sub>2</sub>	H	H	OCH <sub>3</sub>	H	OCH <sub>3</sub>	OCH <sub>3</sub>	Br	
<b>34d</b>	CH <sub>2</sub>	H	OCH <sub>3</sub>	OCH <sub>3</sub>	H	OCH <sub>3</sub>	OCH <sub>3</sub>	Br	
<b>34e, 35e</b>	CH <sub>2</sub>	OCH <sub>3</sub>	H	H	OCH <sub>3</sub>	OCH <sub>3</sub>	OCH <sub>3</sub>	Br	
<b>34f, 35f</b>	CH <sub>2</sub>	H	NO <sub>2</sub>	H	H	H	OCH <sub>3</sub>	Cl	
<b>34g, 35g</b>	CH <sub>2</sub>	H	NO <sub>2</sub>	H	H	OCH <sub>3</sub>	OCH <sub>3</sub>	Br	

compound **34g** showed the highest anti-proliferative activity against most human cancer cell lines, with an  $IC_{50}$  value of 0.02  $\mu$ M. From all compounds, the ten most effective **32b,c**, **33c** and **34a–g** were chosen for further anticancer mechanistic studies. Oxime compound **34f** with nitro substitution at position  $R_3$  exhibited the most potent BRAF<sup>V600E</sup> inhibitory activity ( $IC_{50}$  = 0.9  $\mu$ M), and Oxime **32c** with  $N\text{-CH}_3$  substitution at the  $R_1$  position exhibited the highest EGFR inhibitory activity with an  $IC_{50}$  value of 0.07  $\mu$ M, which was equivalent to the positive control Erlotinib.<sup>59</sup> Later, Masand *et al.* applied the multiple quantitative structure–activity relationships (QSARs) models for the anticancer activity of the compounds **32–35**. The models showed that the internal electronic environment of compounds and a specific combination of nitrogen and oxygen atoms connected by five bonds have an association with the anticancer activity.<sup>60</sup>

Two years later, Qin's research team reported the synthesis of new curcumin-like oxime analogues **36a-h** (Fig. 10) using  $\alpha, \beta$ -unsaturated carbonyl based anticancer compounds. MTT assay by MCF-10A cells showed that all oxime analogues were nontoxic with cell viability of more than 88%. The results of the anti-proliferative assay against above mentioned cell lines indicated that all analogues exhibited strong anti-proliferative activity with  $IC_{50}$  values between 0.02 and 2.7  $\mu$ M. Analogues

**36g** and **36h** were most potent agents. The SAR analysis showed that compounds with a combination of 4-N(CH<sub>3</sub>)<sub>2</sub> and 2-NO<sub>2</sub> groups exhibited considerably potent anticancer activity compared to those having -CH(OCH<sub>2</sub>CH<sub>3</sub>)<sub>2</sub> group at position 4 of rings. The mechanistic study revealed that compounds **36c** and **36d** were the most potent inhibitors of tubulin assembly; compounds **36e** and **36f** were the most potent inhibitors of EGFR, and all compounds were potent inhibitors of BRAF<sup>V600E</sup> with IC<sub>50</sub> values between 1.3–3.1  $\mu$ M.<sup>61</sup>

To progress the new anti-inflammatory agents, Li, Zhang and co-workers designed and synthesized twelve pentadienone oxime ester derivatives, which can be considered as the curcumin analogues (37a-k in Fig. 11). Among all the derivatives, compound 37j showed good anti-inflammatory activity with the highest inhibition of LPS-induced nitric oxide (NO) and IL-6 release in murine monocyte-macrophage RAW 264.7 cells with  $IC_{50}$  values of 6.66 and 5.07  $\mu$ M, respectively. The pro-inflammatory mediators NO and IL-6 have significant roles in the progression of inflammation-related diseases. The SAR analysis revealed that pyridine ring substituent at  $R_3$  is better than that of benzene, and substituent  $R_2$  of benzene possessed a significant influence on inhibition activity.<sup>62</sup>

The synthetic methodology, yields, and distinct biological activity of 32-37 are summarized in Table 9.

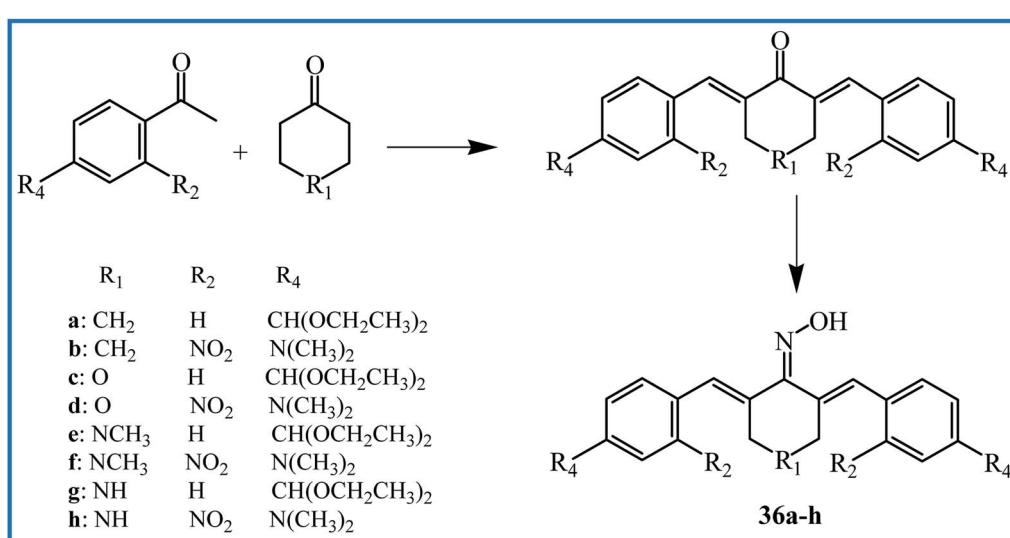


Fig. 10 Synthesis and structure of curcumin-like oxime analogues 36a-h.

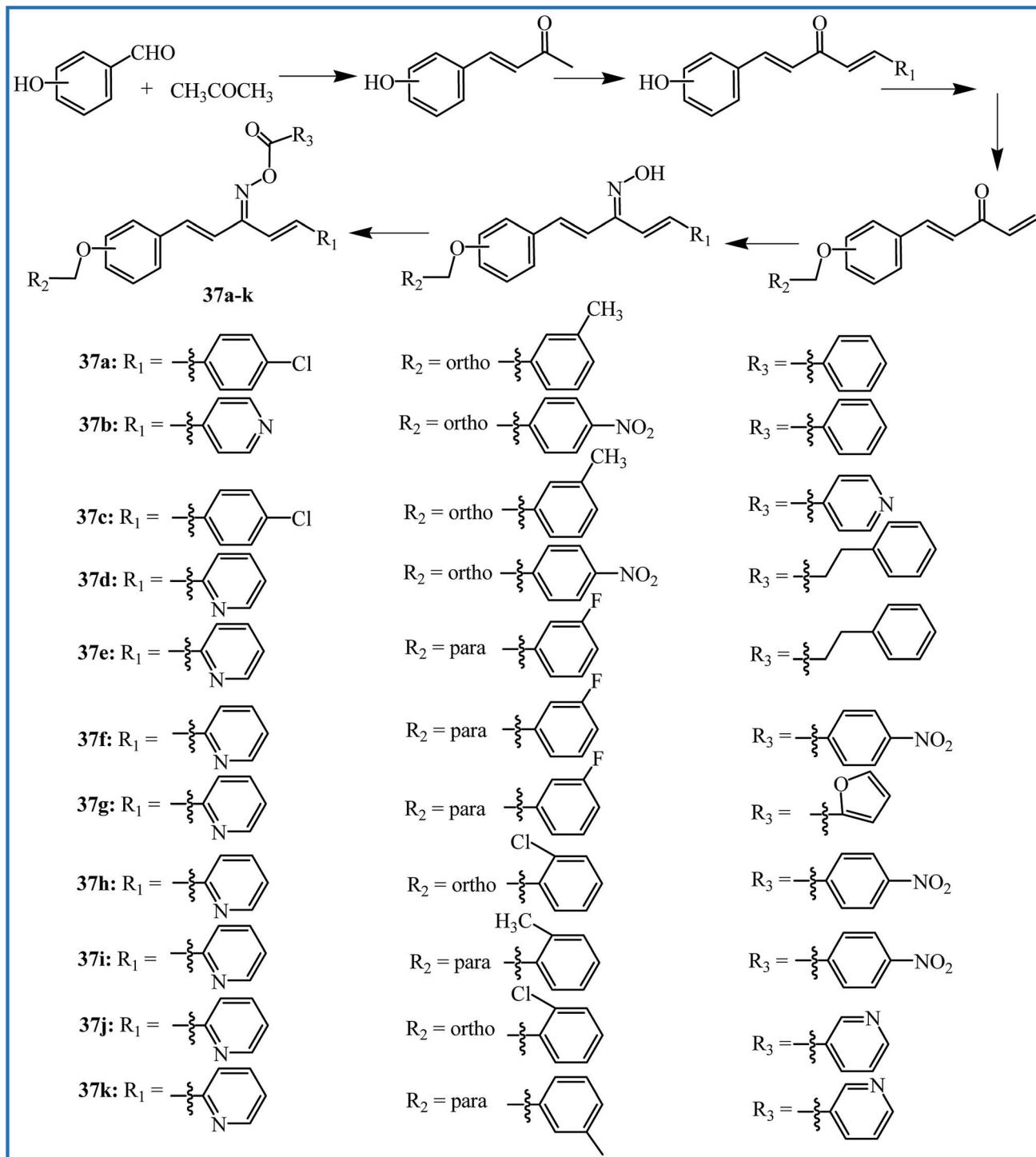


Fig. 11 Synthesis and structure of curcumin-like oxime ester analogues 37a–k.

## 5. Summary and future perspectives

Schiff base reaction is an interesting route for many chemists due to simple, efficient, and high yield protocol. In the last decade, several attempts have been made by many researchers to improve the pharmacological activities of curcumin by Schiff base reaction. The hydroxy and methoxy groups play a vital role

in the antioxidant and anticancer properties of curcumin, and modification of curcumin through carbonyl groups does not interfere with these groups. So, Schiff base reaction is a valuable method to the formation of new curcumin derivatives.

The discussed examples in this review were investigated for antibacterial activity (compounds 1, 2, 8–11, 13–20, and 30), antifungal activity (compounds 2, 9–11, 14–20, and 30),

Table 9 Summary of properties of compounds 32 to 37

Compound	Condition of synthesis	Yield (%)	Activity	Outcome	Reference
32–35	32 and 34: 6–8 h reflux of $\alpha,\beta$ -unsaturated carbonyl compounds with $\text{NH}_2\text{OH}\cdot\text{HCl}$ in EtOH 33 and 35: 8 h reflux of 32 and 34 with haloalkylamine in dry acetone in presence of $\text{K}_2\text{CO}_3$	42–62	Anticancer	34f and 34g were the most potent anticancer agents	60
36a–h	Reflux of $\alpha,\beta$ -unsaturated carbonyl compounds with $\text{NH}_2\text{OH}\cdot\text{HCl}$ in EtOH	39–51	Anticancer	36g and 36h were the most potent anticancer agents	61
37a–k	Stirring of precursors for 5 h at 0–5 °C in dry acetone in presence of $\text{K}_2\text{CO}_3$	48.2–76	Anti-inflammatory	37j was the most potent anti-inflammatory agent	62

antioxidant activity (compounds 4–7, 12, 21, 22, and 31), anti-inflammatory activity (compounds 14–17 and 37), DNA cleavage efficacy (compounds 3, 9, 10, 18–20, and 26–30), and anticancer activity (compounds 5–7, 11, 12, 21–25, 28, 29, 32–36).

For several compounds (4–8, 13–17, 21, 22, 24, 25, and 31), the planned activities have been compared with those of curcumin, and in most of them, an improvement in activity can be seen. This instruction can't apply to antioxidant properties, and compounds 4, 5g–i, 6e–h, 7, 21, 22, and 31 exhibited lower antioxidant activity compared to curcumin. This decrease in antioxidant activity is very notable in compounds 21 and 22 that have been synthesized from a curcumin analogue without hydroxy and methoxy groups on the aromatic rings. Among the compound, only 6a–d exhibited a slightly higher antioxidant activity compared to curcumin.

In several studies, including compounds 1–3, 8–11, 18–20, 29, 30 and 31, the complexes of ligands with various metals such as Cu(II), Ni(II), Co(II), and Zn(II) have also been synthesized. All metal complexes showed improved activities (including antibacterial, antifungal and DNA cleavage) compared to parent ligands. About the antibacterial and anti-fungal activities, the zinc complex of 1 and copper complexes of 2, 3, 8–11, and 18–20 showed the highest activity. The authors explained this advancement of activity by Overtone's concept<sup>63</sup> and the Tweedy's chelation theory.<sup>64</sup> Based on Overtone's concept, the lipophilicity of the cell membrane is a significant factor that controls cell permeability. According to chelation, the overlap of the orbital of ligand and partial distribution of the positive charge of the metal ion with donor groups leads to a principal decrease of the polarity of the metal ion and the increase in the delocalization of  $\pi$ -electrons over the chelate ring. The decreased polarity of the metal ion enhances the lipophilicity and penetration of the complexes into the membrane of the cell. The complexes can block the metal-binding sites in the enzymes of microorganisms and disturb the vital cellular processes such as the respiration process and synthesis of proteins. In most reports, the copper complex shows higher activity than other complexes, which is due to its greater size that decreases the polarization. It is also stated that the enhanced activity of Cu(II) complex can be attributed to effective binding with DNA.<sup>32</sup>

Designing the drug delivery systems that bind to curcumin through Schiff base reaction is a useful strategy because it can result in stimuli-responsive release of curcumin in the target tissue. Cancer microenvironment is reported to have lower pH than the normal tissues, and the Schiff base bond as a dynamic chemical bond can be hydrolyzed in the acidic environment to release curcumin. Therefore, the use of hydrophilic polymers including the amino groups is suggested to develop the stimuli-sensitive delivery systems. These systems not only lead to targeted delivery of curcumin, but can also significantly increase the water-solubility of this compound. It is also apparent from the studies that presence of polar groups including hydroxy and methoxy groups in the introducing amine compound (6a–h) also increases the water-solubility of curcumin.

Comparing the results obtained for 14–17 derivatives indicated that formation Schiff base on both carbonyl groups of curcumin decrease the biological activities. An overview of all compounds also proved that most compounds with outstanding activities (such as 5a–f, 5i, 6a–d, 14b–e, 16a and 23l) have an unblocked carbonyl group.

The results of studies also revealed that the combination of curcumin with other drug families such as sulfonamides leads to a synergistic effect and improves biological properties. It seems that the use of amine compounds containing different pharmacological groups to attach the curcumin by Schiff base reaction can be an effective way to obtain new analogues with improved properties. We complete this review by hoping that it will stimulate researchers to develop the new and different derivatives of curcumin to obtain qualified compounds in anticancer, antimicrobial, antioxidant, and other medicinal and biological fields.

## Conflicts of interest

There are no conflicts of interest.

## Acknowledgements

The authors are appreciative for budgetary help from Iran National Science Foundation (INSF) as well as Lorestan University for facilitations.



## References

- 1 Q. Yao, Z. q. Ke, S. Guo, X. s. Yang, F. x. Zhang, X. f. Liu, X. Chen, H. g. Chen, H. y. Ke and C. Liu, *J. Mol. Cell. Cardiol.*, 2018, **124**, 26–34.
- 2 D. Bagchi, S. Chaudhuri, S. Sardar, S. Choudhury, N. Polley, P. Lemmens and S. K. Pal, *RSC Adv.*, 2015, **5**, 102516–102524.
- 3 A. I. Joseph, R. L. Edwards, P. B. Luis, S. H. Presley, N. A. Porter and C. Schneider, *Org. Biomol. Chem.*, 2018, **16**, 3273–3281.
- 4 X. X. Yang, C. M. Li, Y. F. Li, J. Wang and C. Z. Huang, *Nanoscale*, 2017, **9**, 16086–16092.
- 5 S. Izui, S. Sekine, K. Maeda, M. Kuboniwa, A. Takada, A. Amano and H. Nagata, *J. Periodontol.*, 2016, **87**, 83–90.
- 6 G. Djokeng Paka, S. Doggui, A. Zaghami, R. Safar, L. Dao, A. Reisch, A. Klymchenko, V. G. Roullin, O. Joubert and C. Ramassamy, *Mol. Pharm.*, 2016, **13**, 391–403.
- 7 J. Chen, Z. M. He, F. L. Wang, Z. S. Zhang, X. z. Liu, D. D. Zhai and W. D. Chen, *Eur. J. Pharmacol.*, 2016, **772**, 33–42.
- 8 H. Soleimani, A. Amini, S. Taheri, E. Sajadi, S. Shafikhani, L. A. Schuger, V. B. Reddy, S. K. Ghoreishi, R. Pouriran and S. Chien, *J. Photochem. Photobiol. B Biol.*, 2018, **181**, 23–30.
- 9 M. Qureshi, E. A. Al-Suhaimi, F. Wahid, O. Shehzad and A. Shehzad, *Neurol. Sci.*, 2018, **39**, 207–214.
- 10 F. N. Kaufmann, M. Gazal, C. R. Bastos, M. P. Kaster and G. Ghisleni, *Eur. J. Pharmacol.*, 2016, **784**, 192–198.
- 11 P. Kumaraswamy, S. Sethuraman and U. M. Krishnan, *J. Agric. Food Chem.*, 2013, **61**, 3278–3285.
- 12 R. K. Singh, D. Rai, D. Yadav, A. Bhargava, J. Balzarini and E. De Clercq, *Eur. J. Med. Chem.*, 2010, **45**, 1078–1086.
- 13 M. G. El-Gazzar, N. H. Zaher, E. M. El-Hossary and A. F. Ismail, *J. Photochem. Photobiol. B Biol.*, 2016, **162**, 694–702.
- 14 Y. P. Bharitkar, M. Das, N. Kumari, M. P. Kumari, A. Hazra, S. S. Bhayye, R. Natarajan, S. Shah, S. Chatterjee and N. B. Mondal, *Org. Lett.*, 2015, **17**, 4440–4443.
- 15 M. Singh, A. Hazra, Y. P. Bharitkar, R. Kalia, A. Sahoo, S. Saha, V. Ravichandiran, S. Ghosh and N. B. Mondal, *RSC Adv.*, 2018, **8**, 18938–18951.
- 16 L. Rišiaňová, E. Fischer-Fodor, J. Valentová, C. Tatomir, N. C. Decea, P. Virág, I. Pechová, F. Devínsky and N. Miklášová, *Bioorg. Med. Chem. Lett.*, 2017, **27**, 2345–2349.
- 17 A. Arezki, G. G. Chabot, L. Quentin, D. Scherman, G. Jaouen and E. Brulé, *Med. Chem. Commun.*, 2011, **2**, 190–195.
- 18 F. C. Rodrigues, N. A. Kumar and G. Thakur, *Eur. J. Med. Chem.*, 2019, **177**, 76–104.
- 19 S. A. Noureddin, R. M. El-Shishtawy and K. O. Al-Footy, *Eur. J. Med. Chem.*, 2019, **182**, 111631.
- 20 S. Zhao, C. Pi, Y. Ye, L. Zhao and Y. Wei, *Eur. J. Med. Chem.*, 2019, **180**, 524–535.
- 21 P. Y. Khor, M. F. F. M. Aluwi, K. Rullah and K. W. Lam, *Eur. J. Med. Chem.*, 2019, **183**, 111704.
- 22 M. A. Tomeh, R. Hadianamrei and X. Zhao, *Int. J. Mol. Sci.*, 2019, **20**, 1033.
- 23 M. Thomas, A. Kulandaisamy and A. Manohar, *Int. J. Chem. Tech. Res.*, 2012, **4**, 247–257.
- 24 S. Sumathi, P. Tharmaraj, C. Sheela and R. Ebenezer, *J. Coord. Chem.*, 2012, **65**, 506–515.
- 25 M. Jayandran, M. Haneefa and V. Balasubramanian, *Int. J. Chem. Nat. Sci.*, 2014, **2**, 157–163.
- 26 M. Jayandran, M. Haneefa and V. Balasubramanian, *Indian J. Sci. Technol.*, 2016, **9**, 1–9.
- 27 J. Rajesh, A. Gubendran, G. Rajagopal and P. Athappan, *J. Mol. Struct.*, 2012, **1010**, 169–178.
- 28 M. H. Afsarian, M. Farjam, E. Zarenezhad, S. Behrouz and M. N. S. Rad, *Acta Chim. Slov.*, 2019, **66**, 874–887.
- 29 R. Revathi, D. A. Ananth, A. Rameshkumar and T. Sivasudha, *Asian J. Chem.*, 2015, **27**, 1489–1494.
- 30 R. De Vreese, C. Grootaert, S. D'hoore, A. Theppawong, S. Van Damme, M. Van Bogaert, J. Van Camp and M. D'hooghe, *Eur. J. Med. Chem.*, 2016, **123**, 727–736.
- 31 A. Theppawong, R. De Vreese, L. Vannecke, C. Grootaert, J. Van Camp and M. D'hooghe, *Bioorg. Med. Chem. Lett.*, 2016, **26**, 5650–5656.
- 32 A. Kareem, M. Arshad, S. A. Nami and N. Nishat, *J. Photochem. Photobiol. B Biol.*, 2016, **160**, 163–171.
- 33 N. Raman, T. Chandrasekar, G. Kumaravel and L. Mitu, *Appl. Organomet. Chem.*, 2018, **32**, e3922.
- 34 J. Porkodi and N. Raman, *Appl. Organomet. Chem.*, 2018, **32**, e4030.
- 35 A. Palanimurugan and A. Kulandaisamy, *Asian J. Chem.*, 2018, **30**, 1262–1268.
- 36 A. Kareem, M. S. Khan, S. A. Nami, S. A. Bhat, A. U. Mirza and N. Nishat, *J. Mol. Struct.*, 2018, **1167**, 261–273.
- 37 N. G. Gogoi and J. G. Handique, *J. Chem. Sci.*, 2019, **131**, 74.
- 38 J. Lal, S. K. Gupta, D. Thavaselvam and D. D. Agarwal, *Eur. J. Med. Chem.*, 2013, **64**, 579–588.
- 39 M. Ahmed, M. A. Qadir, M. I. Shafiq, M. Muddassar, Z. Q. Samra and A. Hameed, *Arab. J. Chem.*, 2019, **12**, 41–53.
- 40 M. Ahmed, M. A. Qadir, A. Hameed, M. N. Arshad, A. M. Asiri and M. Muddassar, *Biochem. Biophys. Res. Commun.*, 2017, **490**, 434–440.
- 41 T. Chandrasekar, N. Pravin and N. Raman, *Inorg. Chem. Commun.*, 2014, **43**, 45–50.
- 42 T. Chandrasekar, N. Pravin and N. Raman, *J. Mol. Struct.*, 2015, **1081**, 477–485.
- 43 T. Chandrasekar and N. Raman, *J. Mol. Struct.*, 2016, **1116**, 146–154.
- 44 A. Theppawong, T. Van de Walle, C. Grootaert, M. Bultinck, T. Desmet, J. Van Camp and M. D'hooghe, *ChemistryOpen*, 2018, **7**, 381–392.
- 45 A. Mahal, P. Wu, Z. H. Jiang and X. Wei, *ChemistrySelect*, 2019, **4**, 366–369.
- 46 M. Massaro, R. Amorati, G. Cavallaro, S. Guernelli, G. Lazzara, S. Milioto, R. Noto, P. Poma and S. Riela, *Colloids Surf. B*, 2016, **140**, 505–513.
- 47 S. Pillarisetti, S. Maya, S. Sathianarayanan and R. Jayakumar, *Colloids Surf. B*, 2017, **159**, 809–819.
- 48 T. Saranya, V. Rajan, R. Biswas, R. Jayakumar and S. Sathianarayanan, *Int. J. Biol. Macromol.*, 2018, **110**, 227–233.
- 49 C. Chen, W. Sun, X. Wang, Y. Wang and P. Wang, *Mater. Sci. Eng. C*, 2018, **85**, 88–96.



50 N. Priyadarshini, I. S. Pillai, C. Joel, R. B. Bennie, S. Subramanian and P. Venkatesh, *Indo Am. j. pharm. sci.*, 2015, **2**, 1491–1505.

51 I. Ali, A. Haque, K. Saleem and M. F. Hsieh, *Bioorg. Med. Chem.*, 2013, **21**, 3808–3820.

52 I. Ali, K. Saleem, D. Wesselinova and A. Haque, *Med. Chem. Res.*, 2013, **22**, 1386–1398.

53 P. Jeyaraman, A. Alagaraj and R. Natarajan, *J. Biomol. Struct. Dyn.*, 2020, **38**, 488–499.

54 M. Călinescu, M. Fiastru, D. Bala, C. Mihailciuc, T. Negreanu-Pîrjol and B. Jurcă, *J. Saudi Chem. Soc.*, 2019, **23**, 817–827.

55 C. Canario, S. Silvestre, A. Falcao and G. Alves, *Curr. Med. Chem.*, 2018, **25**, 660–686.

56 D. S. Reddy, M. Kongot, S. P. Netalkar, M. M. Kurjogi, R. Kumar, F. Avecilla and A. Kumar, *Eur. J. Med. Chem.*, 2018, **150**, 864–875.

57 S. Dutta, A. Murugkar, N. Gandhe and S. Padhye, *Metal based drugs*, 2001, **8**, 183–188.

58 D. Simoni, M. Rizzi, R. Rondanin, R. Baruchello, P. Marchetti, F. P. Invidiata, M. Labbozzetta, P. Poma, V. Carina and M. Notarbartolo, *Bioorg. Med. Chem. Lett.*, 2008, **18**, 845–849.

59 H.-L. Qin, J. Leng, C.-P. Zhang, I. Jantan, M. W. Amjad, M. Sher, M. Naeem-ul-Hassan, M. A. Hussain and S. N. A. Bukhari, *J. Med. Chem.*, 2016, **59**, 3549–3561.

60 V. H. Masand, N. N. El-Sayed, M. U. Bambole and S. A. Quazi, *J. Mol. Struct.*, 2018, **1157**, 89–96.

61 H. L. Qin, J. Leng, B. G. Youssif, M. W. Amjad, M. A. G. Raja, M. A. Hussain, Z. Hussain, S. N. Kazmi and S. N. A. Bukhari, *Chem. Biol. Drug Des.*, 2017, **90**, 443–449.

62 Q. Li, J. Zhang, L. Z. Chen, J. Q. Wang, H. P. Zhou, W. J. Tang, W. Xue and X. H. Liu, *J. Enzyme Inhib. Med. Chem.*, 2018, **33**, 130–138.

63 R. Ramesh and S. Maheswaran, *J. Inorg. Biochem.*, 2003, **96**, 457–462.

64 Y. Anjaneyulu and R. P. Rao, *Synth React Inorg Met Org Chem*, 1986, **16**, 257–272.

